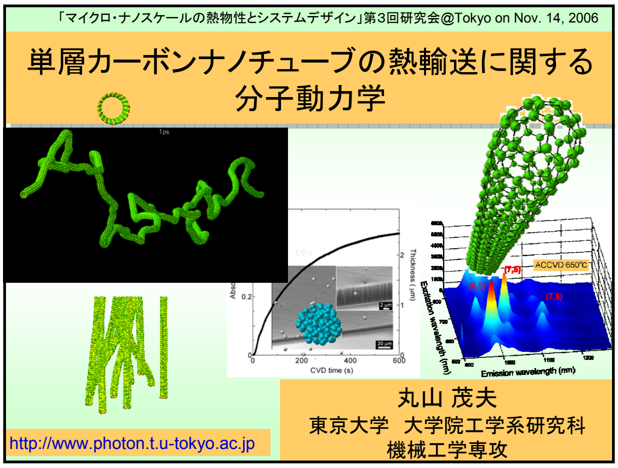
「マイクロ・ナノスケールの熱物性とシステムデザイン」第3回研究会@Tokyo on Nov. 14, 2006
単層カーボンナノチューブの熱輸送に関する
分子動力学
丸山 茂夫
東京大学　大学院工学系研究科
機械工学専攻
http://www.photon.t.u-tokyo.ac.jp

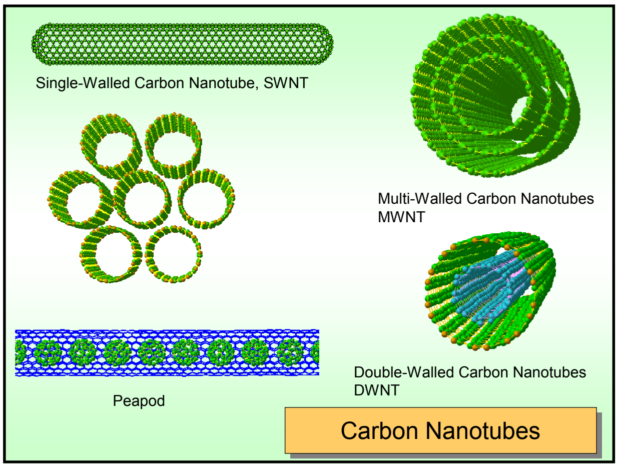
Single-Walled Carbon Nanotube, SWNT
Multi-Walled Carbon Nanotubes
MWNT
Peapod
Double-Walled Carbon Nanotubes
DWNT
Carbon Nanotubes

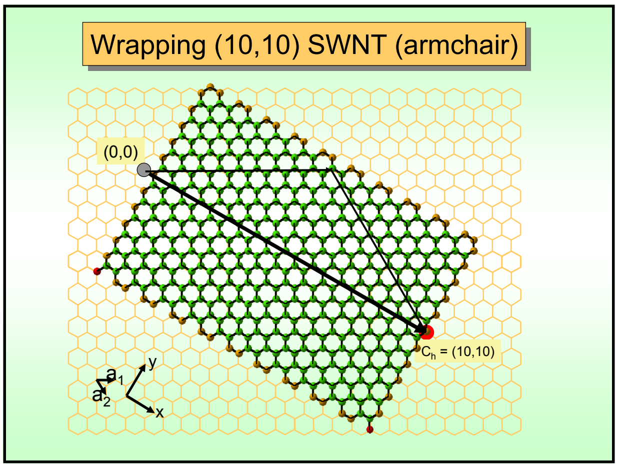
Wrapping (10,10) SWNT (armchair)
(0,0)
C_h = (10,10)
a1
a2
y
x

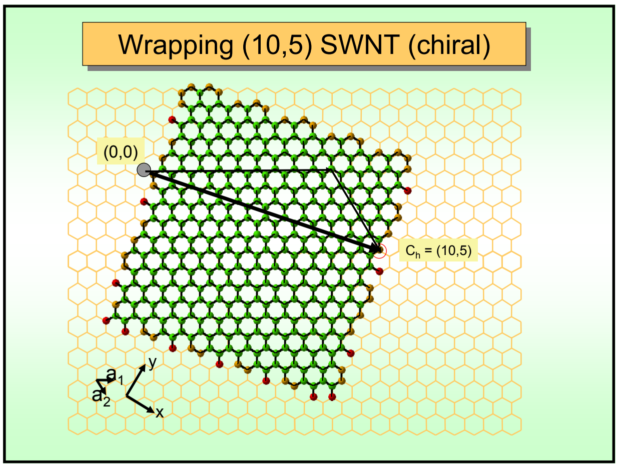
Wrapping (10,5) SWNT (chiral)
(0,0)
C_h = (10,5)
a1
a2
y
x

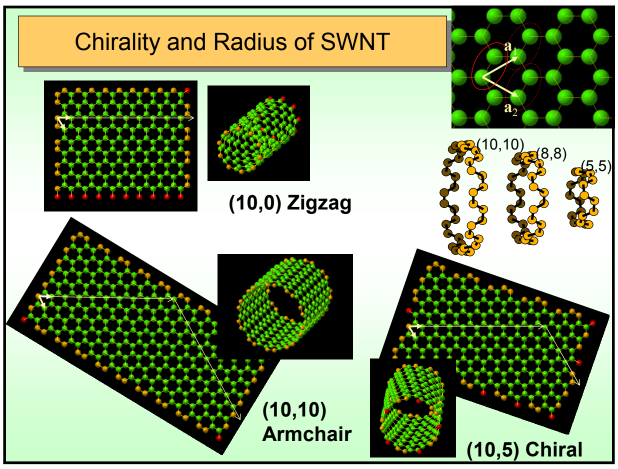
Chirality and Radius of SWNT
(10,0) Zigzag
(10,10)
(8,8)
(5,5)
(10,10)
Armchair
(10,5) Chiral

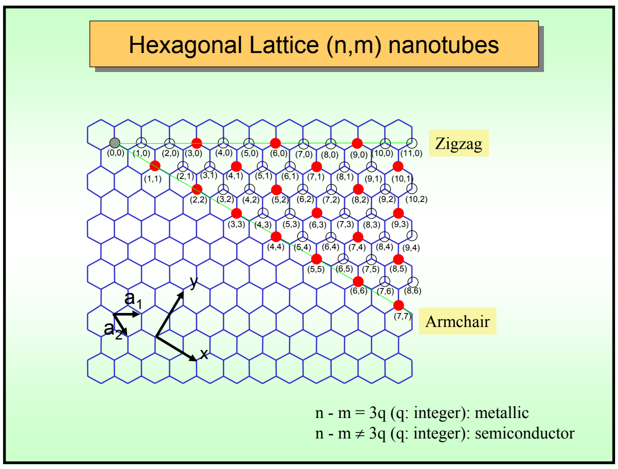
Hexagonal Lattice (n,m) nanotubes
Zigzag
Armchair
a1
a2
y
x
n - m = 3q (q: integer): metallic
n - m ≠ 3q (q: integer): semiconductor

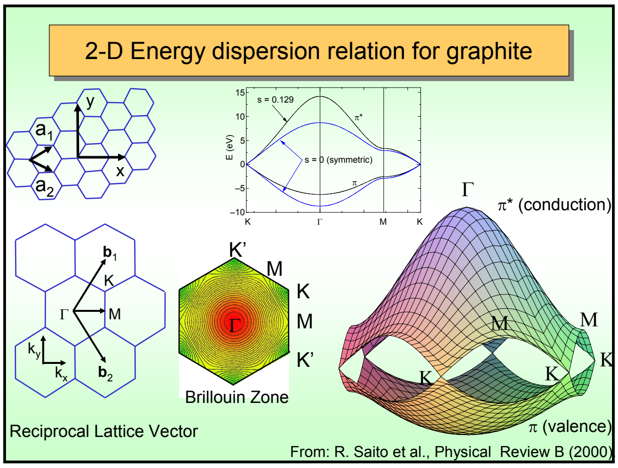
2-D Energy dispersion relation for graphite
y
x
a1
a2
s = 0.129
s = 0 (symmetric)
E (eV)
b1
b2
K
M
Γ
kx
ky
K'
Brillouin Zone
π* (conduction)
π (valence)
Reciprocal Lattice Vector
From: R. Saito et al., Physical Review B (2000)

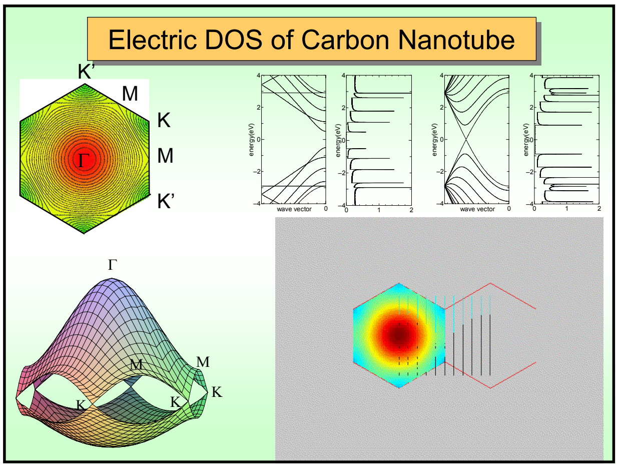
Electric DOS of Carbon Nanotube
K'
M
K
Γ
energy(eV)
wave vector

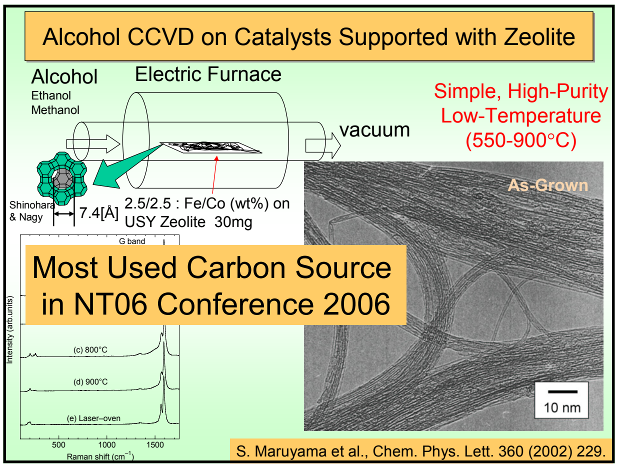
Alcohol CCVD on Catalysts Supported with Zeolite
Alcohol
Ethanol
Methanol
Electric Furnace
vacuum
Simple, High-Purity
Low-Temperature
(550-900°C)
Shinohara & Nagy
7.4[Å]
2.5/2.5 : Fe/Co (wt%) on
USY Zeolite 30mg
As-Grown
Most Used Carbon Source
in NT06 Conference 2006
G band
(c) 800°C
(d) 900°C
(e) Laser-oven
Intensity (arb.units)
Raman shift (cm⁻¹)
10 nm
S. Maruyama et al., Chem. Phys. Lett. 360 (2002) 229.

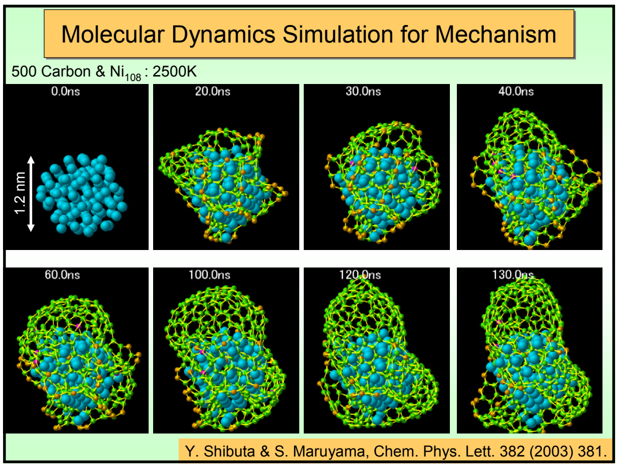
Molecular Dynamics Simulation for Mechanism
500 Carbon & Ni108 : 2500K
0.0ns
20.0ns
30.0ns
40.0ns
1.2 nm
60.0ns
100.0ns
120.0ns
130.0ns
Y. Shibuta & S. Maruyama, Chem. Phys. Lett. 382 (2003) 381.

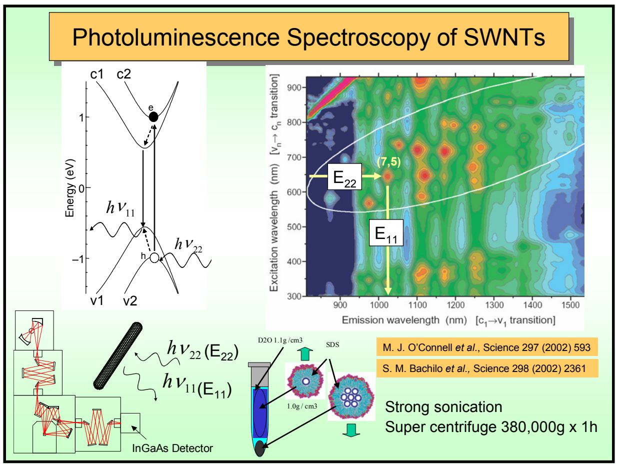
Photoluminescence Spectroscopy of SWNTs
c1 c2
v1 v2
Energy (eV)
hν11
hν22
E22
E11
(7,5)
Excitation wavelength (nm) [vn→cn transition]
Emission wavelength (nm) [c1→v1 transition]
hν22(E22)
hν11(E11)
InGaAs Detector
M. J. O'Connell et al., Science 297 (2002) 593
S. M. Bachilo et al., Science 298 (2002) 2361
Strong sonication
Super centrifuge 380,000g x 1h

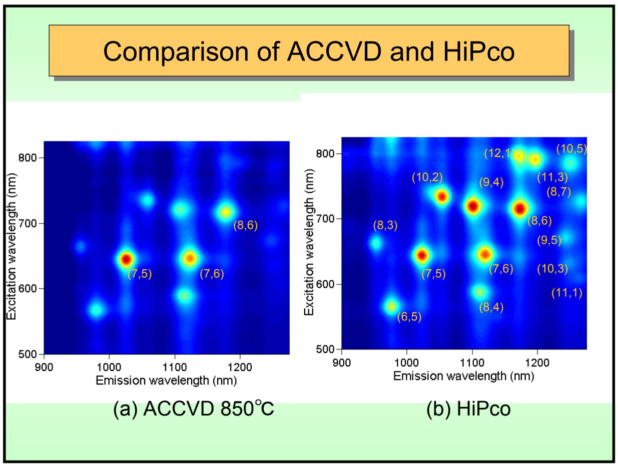
Comparison of ACCVD and HiPco
Excitation wavelength (nm)
Emission wavelength (nm)
(7,5)
(7,6)
(8,6)
(12,1)
(10,5)
(10,2)
(9,4)
(11,3)
(8,7)
(8,3)
(8,6)
(9,5)
(10,3)
(11,1)
(8,4)
(6,5)
(a) ACCVD 850°C
(b) HiPco

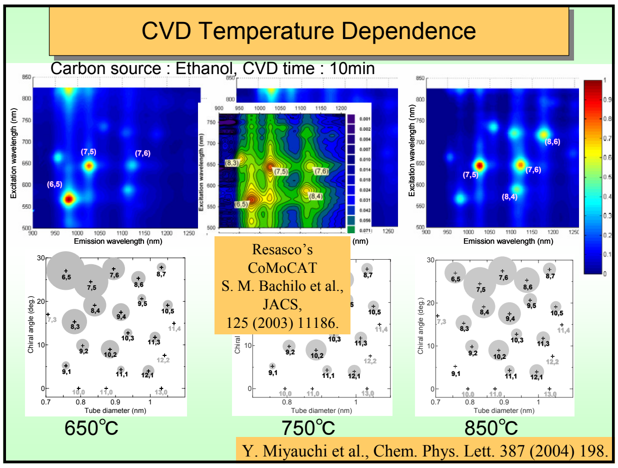
CVD Temperature Dependence
Carbon source : Ethanol, CVD time : 10min
Resasco's
CoMoCAT
S. M. Bachilo et al.,
JACS,
125 (2003) 11186.
650℃
750℃
850℃
Y. Miyauchi et al., Chem. Phys. Lett. 387 (2004) 198.

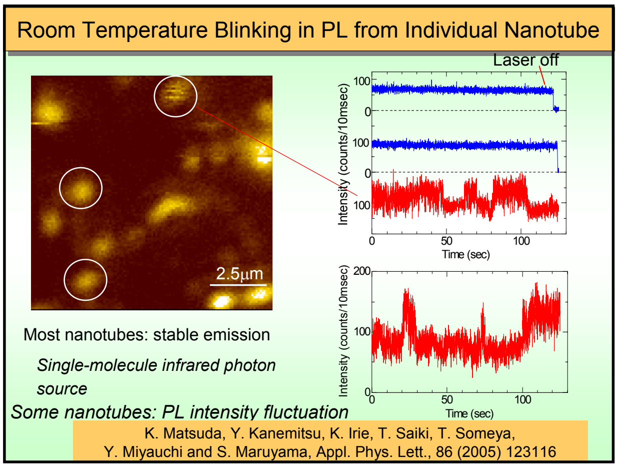
Room Temperature Blinking in PL from Individual Nanotube
Laser off
2.5µm
Intensity (counts/10msec)
Time (sec)
Most nanotubes: stable emission
Single-molecule infrared photon source
Some nanotubes: PL intensity fluctuation
K. Matsuda, Y. Kanemitsu, K. Irie, T. Saiki, T. Someya,
Y. Miyauchi and S. Maruyama, Appl. Phys. Lett., 86 (2005) 123116

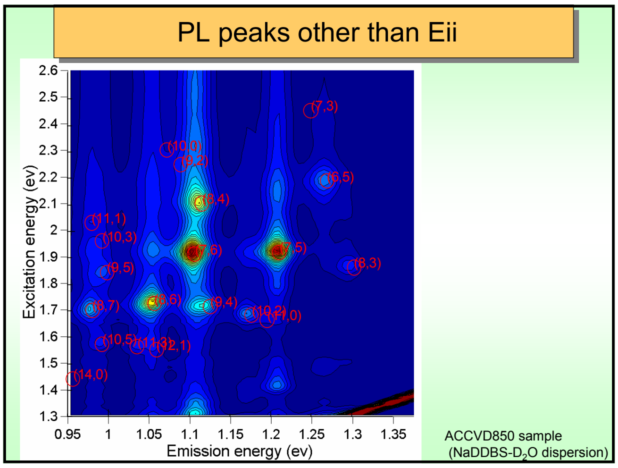
PL peaks other than Eii
Excitation energy (ev)
Emission energy (ev)
ACCVD850 sample
(NaDDBS-D2O dispersion)

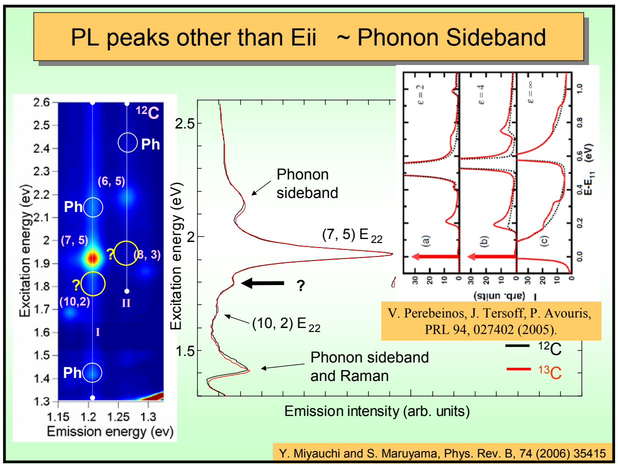
PL peaks other than Eii ~ Phonon Sideband
Excitation energy (ev)
Emission energy (ev)
Excitation energy (eV)
Phonon sideband
(7, 5) E22
(10, 2) E22
Phonon sideband and Raman
Emission intensity (arb. units)
12C
13C
V. Perebeinos, J. Tersoff, P. Avouris,
PRL 94, 027402 (2005).
Y. Miyauchi and S. Maruyama, Phys. Rev. B, 74 (2006) 35415

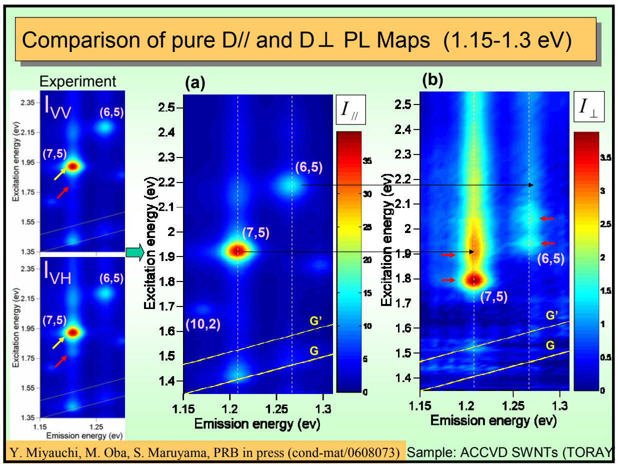
Comparison of pure D// and D⊥ PL Maps (1.15-1.3 eV)
Experiment
(a)
(b)
Excitation energy (ev)
Emission energy (ev)
Y. Miyauchi, M. Oba, S. Maruyama, PRB in press (cond-mat/0608073)
Sample: ACCVD SWNTs (TORAY

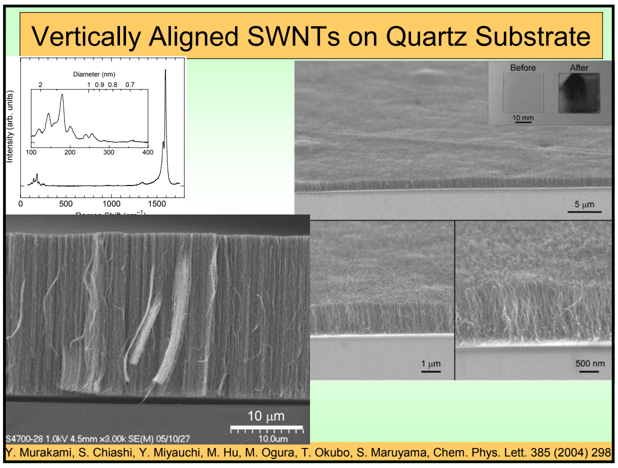
Vertically Aligned SWNTs on Quartz Substrate
Before
After
10 µm
5 µm
1 µm
500 nm
Y. Murakami, S. Chiashi, Y. Miyauchi, M. Hu, M. Ogura, T. Okubo, S. Maruyama, Chem. Phys. Lett. 385 (2004) 298

Detachment of VA-SWNT films with hot water

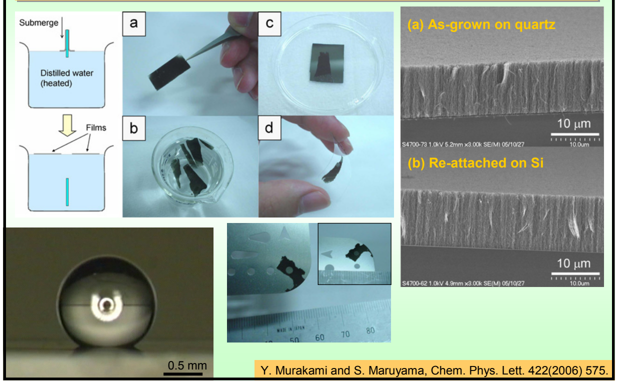

Y. Murakami and S. Maruyama, Chem. Phys. Lett. 422(2006) 575.

TEM Image from Top of Carpet

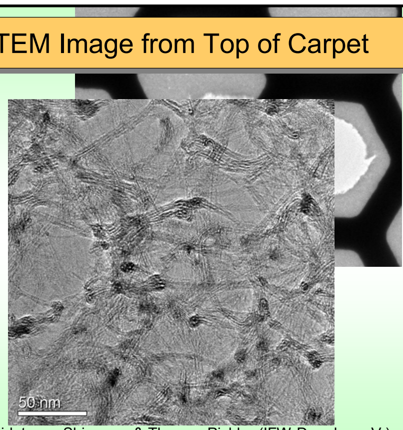

Hidetsugu Shiozawa & Thomas Pichler (IFW-Dresden e.V.),
Erik Einarsson, Shigeo Maruyama

Berber, S., Kwon, Y.-K., Tomanek, D., Phys. Rev. Lett., 84-20 (2000), 4613-4616.

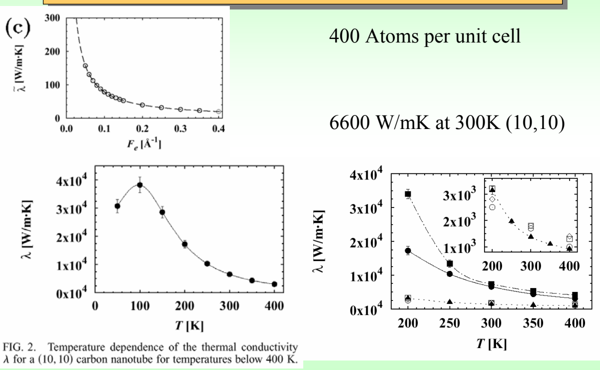

400 Atoms per unit cell

6600 W/mK at 300K (10,10)

FIG. 2. Temperature dependence of the thermal conductivity λ for a (10, 10) carbon nanotube for temperatures below 400 K.

Experimental challenges
Measurement of isolated MWNTs

Temperature dependence

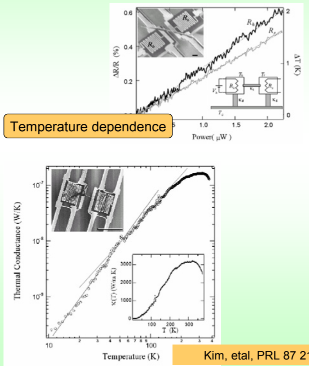

Kim, etal, PRL 87 215502(2001).

Diameter dependence

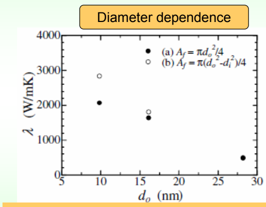

Fujii, etal, PRL 95 065502 (2005).

Experimental measurements of SWNT thermal conductivity

Temperature dependence of suspended SWNTs

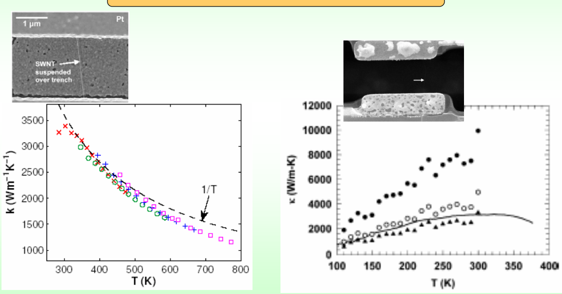

E. Pop *et al*, *Nano Lett.*, 6 (2006) 96

C. Yu *et al*, *Nano Lett.*, 5 (2005) 1842

Tersoff-Brenner Potential

Total Energy E_b:

$$E_b = \sum_i \sum_{j(<i)} \left\{ V_R(r_{ij}) - B^*_{ij} V_A(r_{ij}) \right\}$$

From D. W. Brenner: *Phys. Rev. B*, **42**, 9458(1990)

$$V_R(r) = f(r)\frac{D_e}{S-1}\exp\left\{-\beta\sqrt{2S}(r-R_e)\right\}$$

$$V_A(r) = f(r)\frac{D_e S}{S-1}\exp\left\{-\beta\sqrt{\frac{2}{S}}(r-R_e)\right\}$$

$$B^*_{ij} = \frac{B_{ij}+B_{ji}}{2}, \quad B_{ij} = \left[1 + \sum_{k(\neq i,j)} \left\{ G_c(\theta_{ijk}) f(r_{ik}) \right\} \right]^{-\delta}$$

$$G_c(\theta) = a_0\left(1 + \frac{c_0^{\,2}}{d_0^{\,2}} - \frac{c_0^{\,2}}{d_0^{\,2} + (1+\cos\theta)^2}\right)$$

Potential I
$D_e =$ 6.325 eV $S=$ 1.29 $\beta =$ 1.5Å^{-1} $R_e =$ 1.315Å
$\delta =$ 0.80469 $a_0 =$ 0.011304 $c_0 =$ 19 $d_0 =$ 2.5
$R_1 =$ 1.7Å $R_2 =$ 2.0Å

Potential II
$D_e =$ 6.0 eV $S=$ 1.22 $\beta =$ 2.1Å^{-1} $R_e =$ 1.39Å
$\delta =$ 0.5 $a_0 =$ 0.00020813 $c_0 =$ 330 $d_0 =$ 3.5
$R_1 =$ 1.7Å $R_2 =$ 2.0Å

	Single bonds		Double bonds		Triple bonds	
	Fc(N/m)	Re (Å)	Fc (N/m)	Re (Å)	Fc (N/m)	Re (Å)
Potential I	260	1.56	450	1.33	610	1.20
Potential II	500	1.55	870	1.38	1190	1.29
Experimental	450	1.54	950	1.33	1600	1.20

MD Simulation Technique

Without the Periodic Boundary Condition!!

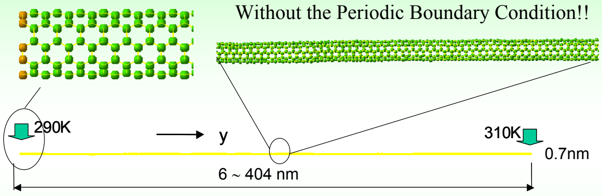

Temperature Control by Phantom Technique

$$m\ddot{\mathbf{x}} = \mathbf{f}_{Pot} + \mathbf{f}_{Rand}(\sigma) - \alpha\,\dot{\mathbf{x}}$$

$$\sigma = \sqrt{2\alpha k_B T_C / \Delta t_S},\ \alpha = m\frac{\pi}{6}\omega_D,\ \omega_D = k_B\theta_D/\hbar$$

$\theta_D = 2500\text{K}$ (Diamond)

Temperature Distribution along a Nanotube

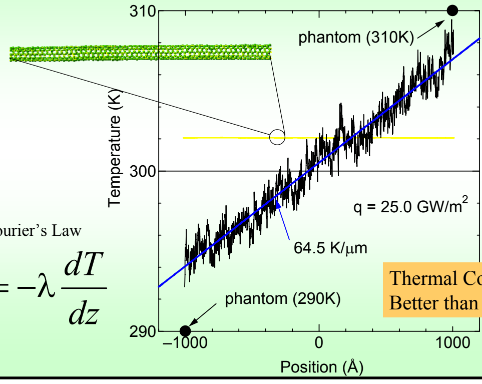

Fourier's Law

$$q = -\lambda\frac{dT}{dz}$$

Thermal Conductivity Better than Diamond?

Effect of Nanotube Length

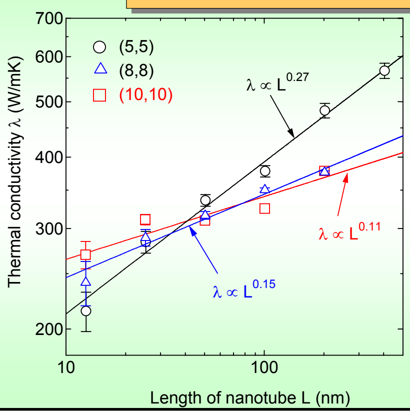

300K

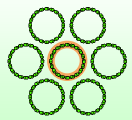

Ring Area of 3.4 Å

Diverging Thermal Conductivity of 1D lattice

FPU (Fermi-Pasta-Ulam) model

S. Lepri, R. Livi and A. Politi,
On the anomalous thermal conductivity of one-dimensional lattices,
Europhys. Lett, 43 (3), 271-276 (1998)

Long wave length Fourier modes $\lambda \propto L^{2/5}$

Diatomic Toda Lattice

Hatano T, Heat conduction in the diatomic Toda lattice revisited,
Phys. Rev. E, 59, R1-R4

Due to long time tail in Green-Kubo Integrands $\lambda \propto L^{0.35}$

Zhang, Fei, Isbister, Dennis J., Evans, Denis J.,
Nonequilibrium molecular dynamics simulations of heat flow in one-dimensional lattices.
Phys. Rev. E, (2000), 61(4-A), 3541-3546.

Evance NEMD makes solitons With high heat flux

Heat in One Dimension in Nature

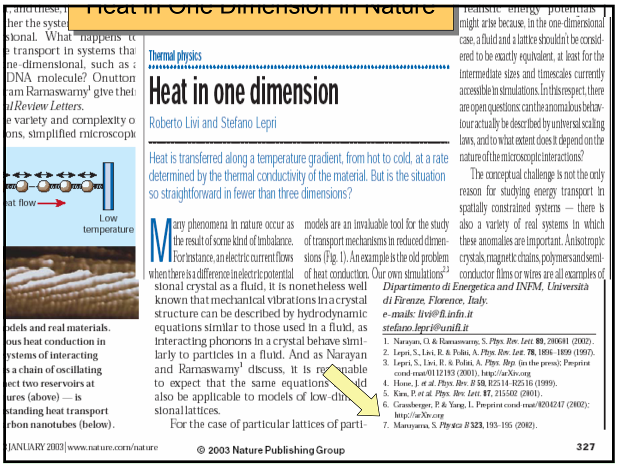

Thermal physics

Heat in one dimension

Roberto Livi and Stefano Lepri

Heat is transferred along a temperature gradient, from hot to cold, at a rate determined by the thermal conductivity of the material. But is the situation so straightforward in fewer than three dimensions?

Many phenomena in nature occur as the result of some kind of imbalance. For instance, an electric current flows when there is a difference in electric potential

models are an invaluable tool for the study of transport mechanisms in reduced dimensions (Fig. 1). An example is the old problem of heat conduction. Our own simulations[2,3]

sional crystal as a fluid, it is nonetheless well known that mechanical vibrations in a crystal structure can be described by hydrodynamic equations similar to those used in a fluid, as interacting phonons in a crystal behave similarly to particles in a fluid. And as Narayan and Ramaswamy[1] discuss, it is reasonable to expect that the same equations should also be applicable to models of low-dimensional lattices.

For the case of particular lattices of parti-

might arise because, in the one-dimensional case, a fluid and a lattice shouldn't be considered to be exactly equivalent, at least for the intermediate sizes and timescales currently accessible in simulations. In this respect, there are open questions: can the anomalous behaviour actually be described by universal scaling laws, and to what extent does it depend on the nature of the microscopic interactions?

The conceptual challenge is not the only reason for studying energy transport in spatially constrained systems — there is also a variety of real systems in which these anomalies are important. Anisotropic crystals, magnetic chains, polymers and semiconductor films or wires are all examples of

Dipartimento di Energetica and INFM, Università di Firenze, Florence, Italy.
e-mails: livi@fi.infn.it
stefano.lepri@unifi.it

1. Narayan, O. & Ramaswamy, S. *Phys. Rev. Lett.* **89**, 200601 (2002).
2. Lepri, S., Livi, R. & Politi, A. *Phys. Rev. Lett.* **78**, 1896–1899 (1997).
3. Lepri, S., Livi, R. & Politi, A. *Phys. Rep.* (in the press); Preprint cond-mat/0112193 (2001). http://arXiv.org
4. Hone, J. *et al. Phys. Rev. B* **59**, R2514–R2516 (1999).
5. Kim, P. *et al. Phys. Rev. Lett.* **87**, 215502 (2001).
6. Grassberger, P. & Yang, L. Preprint cond-mat/0204247 (2002); http://arXiv.org
7. Maruyama, S. *Physica B* **323**, 193–195 (2002).

JANUARY 2003 | www.nature.com/nature © 2003 Nature Publishing Group 327

Length dependence of finite-length SWNT thermal conductivity (2)

Linearized Boltxmann-Peierls phonon transport eqn.

"Divergence disappears if considering second order (or higher) 3-phonon scattering processes"

Mingo and Broido, Nano Letters 5(7) 1221 (2005)

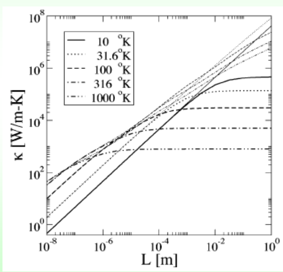

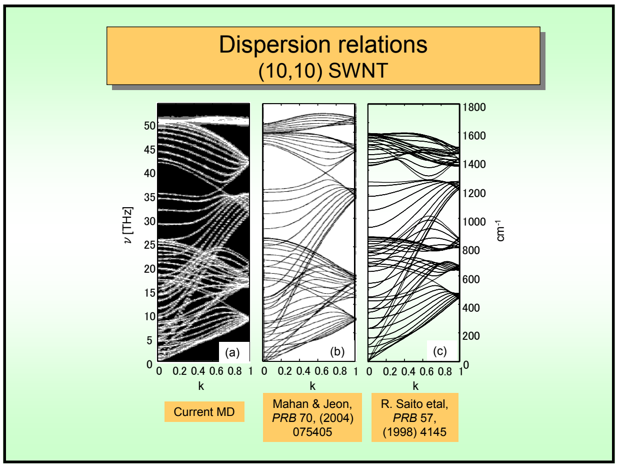
Dispersion relations
(10,10) SWNT
ν [THz]
cm⁻¹
k
(a)
(b)
(c)
Current MD
Mahan & Jeon, PRB 70, (2004) 075405
R. Saito etal, PRB 57, (1998) 4145

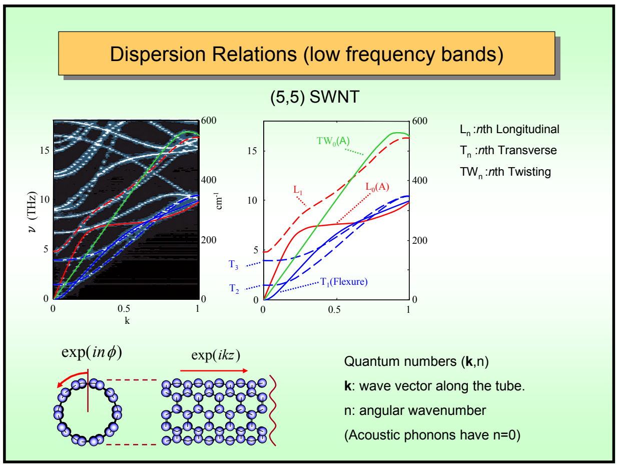
Dispersion Relations (low frequency bands)
(5,5) SWNT
ν (THz)
cm⁻¹
k
TW0(A)
L1
L0(A)
T3
T2
T1(Flexure)
Ln :nth Longitudinal
Tn :nth Transverse
TWn :nth Twisting
exp(inφ)
exp(ikz)
Quantum numbers (k,n)
k: wave vector along the tube.
n: angular wavenumber
(Acoustic phonons have n=0)

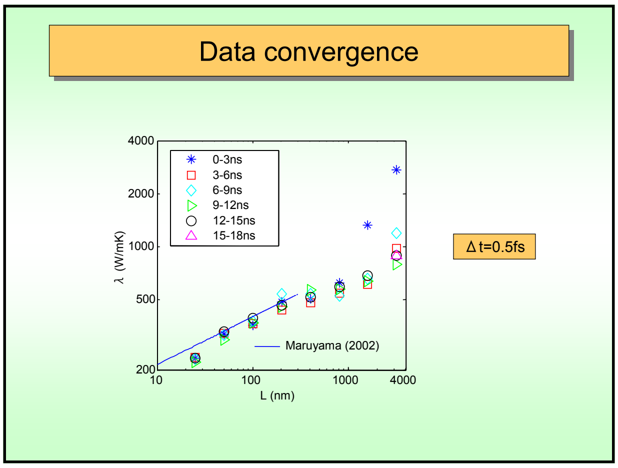
Data convergence
λ (W/mK)
L (nm)
0-3ns
3-6ns
6-9ns
9-12ns
12-15ns
15-18ns
Maruyama (2002)
Δt=0.5fs

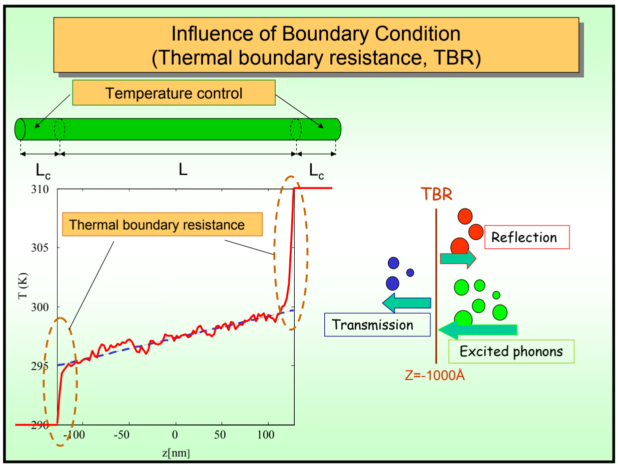
Influence of Boundary Condition
(Thermal boundary resistance, TBR)
Temperature control
Lc
L
Lc
Thermal boundary resistance
T (K)
z[nm]
TBR
Reflection
Transmission
Excited phonons
Z=-1000Å

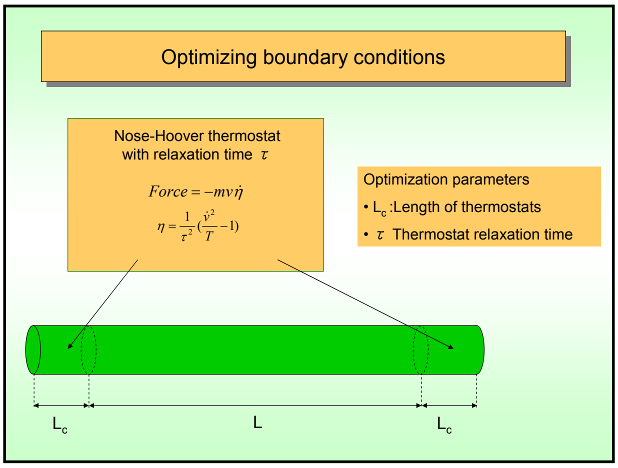
Optimizing boundary conditions
Nose-Hoover thermostat
with relaxation time τ
Force = −mvη̇
η̇ = 1/τ² (v²/T − 1)
Optimization parameters
• Lc :Length of thermostats
• τ Thermostat relaxation time
Lc
L
Lc

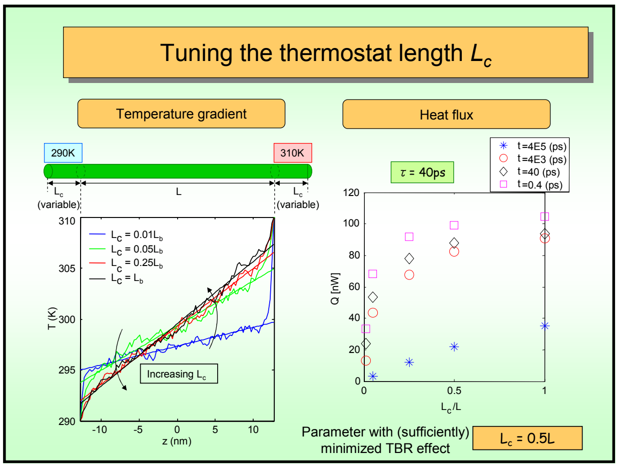
Tuning the thermostat length Lc
Temperature gradient
Heat flux
290K
310K
Lc (variable)
L
Lc (variable)
Lc = 0.01Lb
Lc = 0.05Lb
Lc = 0.25Lb
Lc = Lb
Increasing Lc
T (K)
z (nm)
τ = 40ps
t=4E5 (ps)
t=4E3 (ps)
t=40 (ps)
t=0.4 (ps)
Q [nW]
Lc/L
Parameter with (sufficiently) minimized TBR effect
Lc = 0.5L

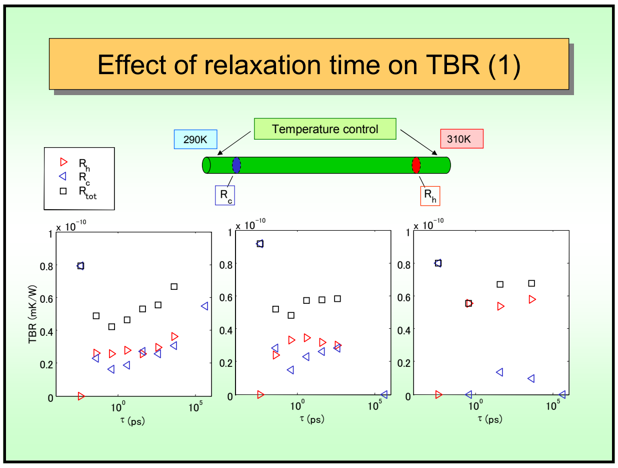
Effect of relaxation time on TBR (1)
Temperature control
290K
310K
R_c
R_h
R_h
R_c
R_{tot}
TBR (mK/W)
τ (ps)

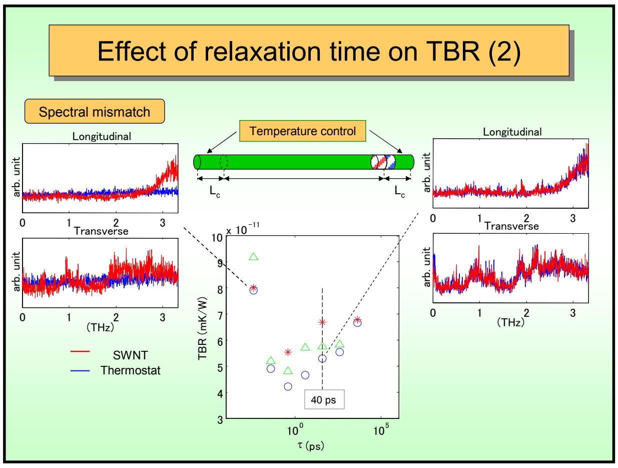
Effect of relaxation time on TBR (2)
Spectral mismatch
Longitudinal
Transverse
arb. unit
(THz)
SWNT
Thermostat
Temperature control
L_c
L_c
TBR (mK/W)
40 ps
τ (ps)

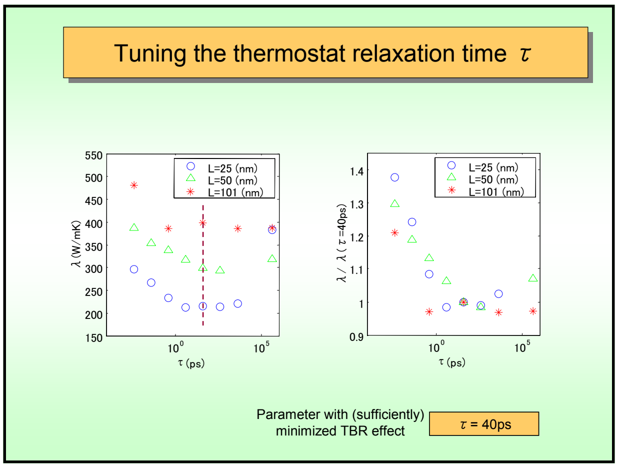
Tuning the thermostat relaxation time τ
L=25 (nm)
L=50 (nm)
L=101 (nm)
λ (W/mK)
λ / λ (τ=40ps)
τ (ps)
Parameter with (sufficiently) minimized TBR effect
τ = 40ps

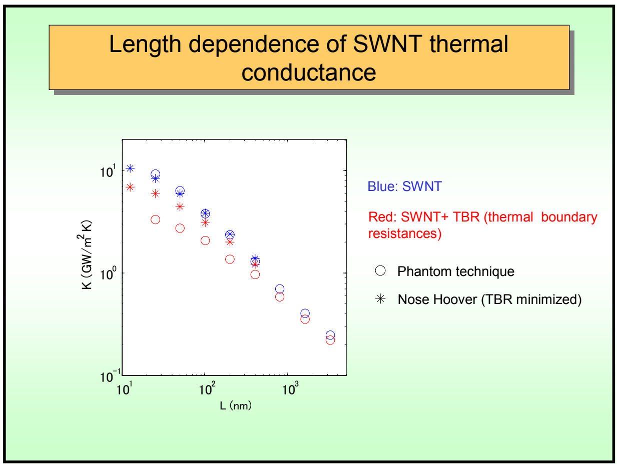
Length dependence of SWNT thermal conductance
K (GW/m²K)
L (nm)
Blue: SWNT
Red: SWNT+ TBR (thermal boundary resistances)
Phantom technique
Nose Hoover (TBR minimized)

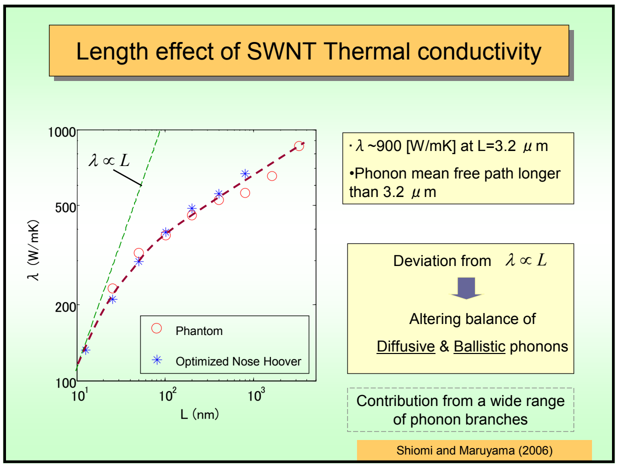
Length effect of SWNT Thermal conductivity
$\lambda \propto L$
λ (W/mK)
L (nm)
Phantom
Optimized Nose Hoover
· λ ~900 [W/mK] at L=3.2 μm
•Phonon mean free path longer than 3.2 μm
Deviation from $\lambda \propto L$
Altering balance of
Diffusive & Ballistic phonons
Contribution from a wide range of phonon branches
Shiomi and Maruyama (2006)

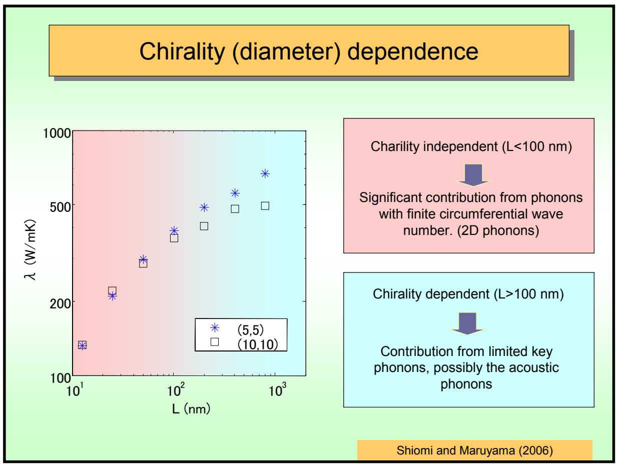
Chirality (diameter) dependence
λ (W/mK)
L (nm)
(5,5)
(10,10)
Charility independent (L<100 nm)
Significant contribution from phonons with finite circumferential wave number. (2D phonons)
Chirality dependent (L>100 nm)
Contribution from limited key phonons, possibly the acoustic phonons
Shiomi and Maruyama (2006)

Summaries

- Thermal conductivity was measurement by minimizing the influence of tube-ends boundary resistances for comparisons with theories and experiments.
- Thermal conductivity was measured up to 3.2 μm and the maximum value was about 800 W/mK, about 1/4 of the experimentally observed value.
- Length dependence of SWNT was identified.
  - ◊ Short nanotubes: diffusive-ballistic transport of a range of phonon branches
  - ◊ Long nanotubes: Ballistic transport of the key phonons
- Diameter independence of the thermal conductivity in (L<200 nm) suggests active contribution from 2D phonons in the regime

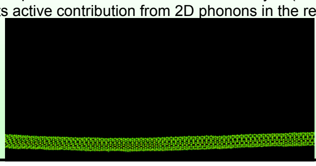

Non-Fourier heat conduction in SWNT

$$1.\ \tau\frac{\partial^2 T}{\partial t^2}+\frac{\partial T}{\partial t}=\alpha\nabla^2 T$$

$$2.\ \tau_q\frac{\partial^2 T}{\partial t^2}+\frac{\partial T}{\partial t}=\alpha\left(\nabla^2 T+\tau_\theta\frac{\partial}{\partial t}\nabla^2 T\right)$$

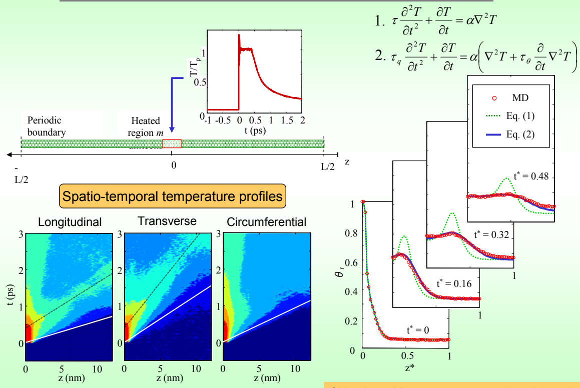

Shiomi and Maruyama, *PRB*, **73** (2006) 205420

Heat conduction of SWNT isotope-superlattices

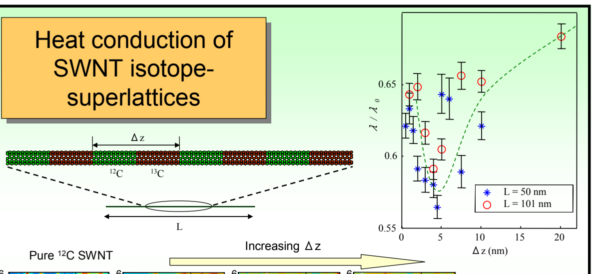

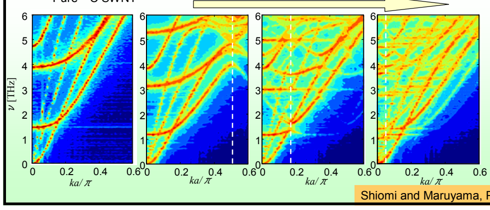

Highlighting molecular dynamics by installing isotopes with double the mass

Shiomi and Maruyama, PRB 74 (2006) 155401.

Professor Richard E. Smalley at Rice University (1943-2005)

1943: Born in Akron, Ohio on June 6
1976: PhD from Princeton,
Assistant Professor at Rice
Laser Vaporization Cluster Beam
1984: Discovery of C60
1996: Nobel Prize in Chemistry with Kroto and Curl
1996: Bulk Production of SWNTs
Then HiPco Process
2000: Testified for National Nanotechnology Initiative
2000: Found Carbon Nanotechnology Inc.
Application of Nanotechnology to Energy Problem
2005: Died at 62 on October 28, 2005